Spokesman: M. Atac
Fermilab

A NEW EXTERNAL HADRON IDENTIFIER DETECTOR

Abstract

In the following, we propose a dE/dx and transition radiation detector to identify hardons at all energies. dE/dx detection covers energies up to 150 GeV/c and transition radiation covers beyond this energy. A prototype detector of this type was built and tested successfully. The detector is composed of 129 layers of 12 μm aluminum foils and 128 multiwire proportional planes. The signal wires grouped together depending on the hadron multiplicities.

A. Oganessian
Yerevan Physics Institute
Armenia, U.S.S.R.

and

M. Atac
Fermilab

17 pgs.

The identification of hadrons in the energy range between 30 GeV/c and 400 GeV/c by means of conventional methods (Cerenkov counters, counters based on the relativistic rise of ionization losses and known versions or x-ray transition radiation (XTR)-detectors) is known to be a rather difficult and even impractical task.

Recently encouraging tests of the external particle identification (EPI) system based on detecting the relativistic rise in ionization have been made at CERN[1] and ISIS system at Fermilab.[2] Such a system would have 8m length[3] and is capable of separating $\pi/k/p$ in the momentum range between 20 and 100 GeV/c. However, identifying fast particles at the higher momenta measuring the energy they lose in the conventional proportional counters is complicated by the combined effect of the slow relativistic rise giving little difference between masses and the broad energy loss spectrum giving poor resolution. Even the multi-hundred stacks of the proportional counters such detectors would be able to identify the hadrons only up to 100-150 GeV/c.

Indeed, it is well known that the most probable ionization losses of the relativistic particles in the absorbers described by the formulae[4]

$$\frac{dE}{dx} = At\left[B + 2\ \ell n\ \frac{E}{mc^2} + \ell n\ At - \delta\right] \qquad (1)$$

where

$$A = 0.154\ Z/A\ \text{MeV}/(\text{gr}/\text{cm}^2)\ ,$$

$$B = \ell n\ m_R c^2\ [10^6\ \text{GeV}]/I,$$

I = mean ionization potential,

t = the thickness of the absorber

δ = the term which takes into account the density effect of the medium.

As it follows from theoretical predictions and from experimental investigation at $4 \lesssim \gamma = E/mc^2 \leq \gamma_1$, δ is very close to zero and relativistic rise is steeper than at $\gamma_1 \leq \gamma \leq \gamma_2$ = (ionization energy)/(plasma energy) and there is a flat region beyond the region of the rise ($\gamma > \gamma_2$) no further increase takes place (Fermi plateau). The values γ_1 and γ_2 depend on the nature of absorber and its density: the smaller density, the higher values γ_1 and γ_2. In the gases at NTP $\gamma_1 \sim$ 40-50 and $\gamma_2 \sim$ 500-1000. The influence of the density effect represents Fig. 1a where the most probable energy losses in xenon are plotted for various pressures. The lower curve corresponds to the ionization losses in arbitrary units at NTP according to Allison, et al.[2] The middle curve represents the prediction of Sternheimer[4] at the pressure of 20 torr. At low pressures the Fermi plateau is shifted to higher energies as shown in Fig. 1a. Evidently the proportional counters at reduced pressure will be capable of separating π's, k's and p's at the higher momenta than the conventional chambers operating at atmospheric pressures.

However, a new method based on x-ray transition radiation shows considerable promise for particle identification. Its merit is that the intensity of this radiation increases linearly with Lorentz factor of the particle. Garibian showed that the energy of the

x-ray transition radiation emitted per unit frequency at the interface between vacuum and dense medium is (5)

$$\frac{dW}{d\omega} = \frac{2}{137\,\pi}\left[\left(0.5 + \frac{\omega^2}{\omega_p^2\gamma^2}\right)\ln\left(1 + \frac{\omega_p^2\gamma^2}{\omega^2}\right) - 1\right] \qquad (2)$$

where $\omega_p = 4\pi Ne^2/m_e$ is the plasma frequency of the medium, N is the number of electrons in 1 cm^3 and e and m_e are the charge and mass of the electron.

The total energy in the x-ray region is

$$W = \frac{2\omega_p}{3\cdot 137\pi}\,\gamma \qquad (3)$$

which we notice is linearly proportional to γ.

However, as it followed from Eqs. (2) and (3), the probability to emit a transition radiation quanta from a single interface is very small. The gain in intensity is possible by using a stack of radiators. In this case the Eqs. (2) and (3) for each interface are valid if fulfilled the expression

$$Z_v = \frac{2\pi c}{\omega\left(\gamma^{-2} + \frac{\omega_p^2}{\omega^2}\right)} < b, \qquad (4)$$

where Z_v is the formation zone of the XTR in the vacuum and b is the air space between the layers.

The XTR detectors based on the energy deposition are recognized at the moment as the most optimum ones. These detectors contain a great number of sections (up to 30[6]) each consisting in its turn of a XTR radiator and a multiwire proportional chamber for the detection of both the ionization and the produced transition radiation.

The signal proportional to the total energy deposition due to ionization losses W_I and the absorption of transition radiation quanta in the chamber gas W_{TR} is formed in each of these chambers at the passage of particles through the detector. If $W = W_I + W_{TR} \gtrsim 1.2W_I$ then, as evidenced by practice, it is possible to identify the particle with a reasonable number of detector sections. However, the condition $W \gtrsim 1.2W_I$ in all the known versions of XTR detectors is met by a number of reasons only at $\gamma \gtrsim 2.10^3$ which in the case of $\pi/k/p$-identification corresponds to momenta $\gtrsim$ 300 GeV/c.

At Yerevan Physics Institute a novel XTR-detector was proposed[7] which is based on the method of the energy deposition and it is capable of the identification of hadrons in the momentum range $30 \leq p \leq 400$ GeV/c. In the proposed detector, the XTR radiator and proportional chambers were combined to reduce the probability of the absorption of transition radiation within the radiator and to increase the number of quanta absorbed in the gas mixture. This fact, together with the choice of the reduced pressure of the filling gas of the chamber allowed to increase the share of the transition radiation in the total energy deposition in the gas mixture.

Such XTR-detector was made at Yerevan Physics Institute and investigated at the Fermi National Accelerator Laboratory. The experimental layout and chamber are shown in Fig. 2. The chamber consists of 18 sensitive planes separated by double-side coated aluminized mylar. The mylar has a thickness of 5 μm and the thickness of aluminum on each side of the mylar is 250 Å. The diameter of sense wires is 25 μm and spacing is 2 mm. All planes were

mounted in a stainless steel gas enclosure with mylar windows. The typical pressure of the gas mixture (80% Xe + 20% CO_2) was 20 ÷ 30 mm Hg.

All signal wires were connected together to the input of a low noise charge sensitive preamplifier. The signal was carried from preamplifier to the amplifier and further to the multichannel pulse height analyzer. The gate of the latter at 40 GeV/c run was triggered by coincidence (or anti-coincidence) between the scintillator telescope ($S1 \cdot S2 \cdot S3 \cdot S4 \cdot \bar{V}$) and the threshold Cerenkov counter. During the 100 GeV/c and 200 GeV/c runs, analyzer was triggered by coincidence between the telescope and differential Cerenkov counter (for the proton runs) or DISC (for the pion run). The proton and pion runs took turns every other hour to eliminate a possible electronic drift. An Fe^{55} x-ray source was used between accelerator cycles to measure variations of the gas gain. A typical Fe^{55} spectrum is shown in Fig. 3.

Figures 4,5, and 6 show the pulse height distributions for pions and protons at 40, 100, and 200 GeV/c respectively, at the pressure of the gas mixture 20 mm Hg. All data were corrected for systematic drifts using Fe^{55} measurements. They show that all the distributions have almost Gaussian shape without long "Landau tail" except for the 200 GeV/c proton run. The explanation of this phenomena probably is that the ionization δ-electrons liberated by the incident particle which are the cause of the long "Landau tail" are captured by dense mylar foils without significant ionization of the gas. The wider distributions at 100 GeV/c and 200 GeV/c are the result of a) the increasing of the XTR share in the total energy yield in the gas, and b) two mylar planes

failed. Figures 3 thru 5 make it clear that at the pressure 20 mm π/P separation is on the order of a full width at half maximum.

Figure 1a represents how the most probable value of the energy deposition in a single cell of the XTR-detector behaves as a function of Lorentz-factor $\gamma = E/mc^2$, at the different conditions. The lower curve corresponds the ionization losses in arbitrary units at NTP according to Allison, et al.[2] The middle curve represents the prediction of Sternheimer[5] at the pressure 20 mm Hg. The dashed curve takes into account XTR contribution. In contrast to case of atmospheric pressure, the reduced pressure shifted Fermi plateau to higher energies as it follows from Fig. 7a. Additional rise in the energy dependence comes from XTR in the Lorentz-factor region $\gamma > 2 \cdot 10^2$. Our experimental data (open circles) are in agreement with the theoretical predictions.

As was to be expected, both the low pressure and XTR allowed to improve the ratio of ionization (peak position) between protons and pions. Indeed, as shown in Fig. 1b, the ratio of ionization W_π/W_p in the xenon at NTP (solid curve) is smaller than at the low pressure (dashed curve). Meanwhile, in this detector W_π/W_p is not only higher, but at $p > 100$ GeV/c, it begins to increase (open circles).

Using the experimental results presented in Figs. 4 thru 6, a Monte Carlo program was simulated for 10 above described XTR-detector samples. To improve the mass resolution, we discarded the largest 4 pulse heights and therefore we took the mean of this set of 6 pulse heights for each particle. An equal number of protons and pions was assumed. Figures 7a, 8 and 9 show the separation of pions and protons achieved this way. The overlapping areas of the proton and pion distributions are about 4-7% at all measured energies.

Figure 7b shows the mean of the 6 smallest signals expected from such a device in the case of the mixture of pions and protons in the ratio 10:1 at 40 GeV/c. The optimum cut between pions and protons would result in a loss of about 12% protons into the pion peak and 12% pions mis-identified as protons. Finally, we note, that the overlapping area is roughly 0.5% in the case of 20 XTR-detector samples for a total length of about 2 m.

Our results suggest that at the momenta $p < 100$ GeV/c, the new XTR-detector is as applicable as Cerenkov counters with the exploitation of ionization losses in MWPC. At the higher energies when these techniques are often inapplicable, XTR-detector becomes more profitable.

Taking into account Monte Carlo predictions and our experimental investigation, we propose a XTR-detector designed for identification of fast secondary particles emerging from Fermilab 30-inch hydrogen bubble chamber. The XTR-detector will efficiently distinguish between protons and pions up to about 300 GeV/c and pions and kaons up to about 450 GeV/c. The detector should have a good multiparticle detection efficiency. The detection area of the first quarter-scale version is assumed to be about 90 cm wide and 45 cm high. A sketchy view of the XTR-detector is shown in Fig. 10. The beam particles passes through 128 cm long drift chamber system normal normal the wire planes. Each plane is sandwiched between two 12μm aluminum (or aluminized mylar) foil drift electrodes which are at the same time the XTR radiators. The wire plane consist of 25 μm thick signal wires and of 75 μm drift wires to provide uniformity of the field and to reduce capacitive cross coupling. The electrostatic field of the

individual planes is perfectly symmetrical, therefore, no forces are exerted either on the wires or on the foils. Each group of 6 signal wires are connected together to the input of a low noise charge sensitive amplifier. It collects the charge from 8 wire planes, so that each particle traversing the detector would yield 16 pulse heights. It means that particle traverses through the 16 groups of cells and every one of them has the cross section 6 x 6 cm and the length 8 cm. Using the data of Aderholz, et al[3] we estimate that such a detector will provide a better multiparticle efficiency than 8 m length of External Particle Identifier (EPI) for BEBC.

The XTR-detector modules, that is both wire and foil planes, will be stacked together inside a stainless steel enclosure with the mylar windows at each end. There will be no pressure difference between the modules. The metallic box will also provide the electrostatic shielding. A study will be done in order to find a gas mixture and its pressure with a suitable slope of the relativistic rise and high voltage characteristics. However, it seems that either the mixture which we have used, i.e., 80% Xe + 20% CO_2 at the pressure of 20-30 mm; or pure propane at the pressure of 60-80 mm will be most proper. It may be necessary to have a pressure regulator system to maintain the pressure of the gas mixture. Probably in case of using the xenon, we may need a gas purification system. We would like to note that although xenon is the most expensive gas, we need about 25 liters to provide the given pressure.

The pulse heights from 16 amplifiers will be stored in ADC's in CAMAC and transferred to a computer for off-line analysis. The Detector Development Group has most of the electronics for the tests.

The essential technical parameters of the XTR-detector could be summarized as follows:

-- effective detection surface 48 x 96 cm^2

-- number of layers (1 cm thick) 128

-- number of active cells per layer 16

-- number of active cells along the particle trajectory 16

-- cell size 6 x 6 x 8 cm^3

-- overall length of the detector is about 1.5 m

-- inside dimensions of the gas enclosure about 70 cm x 120 cm x 150 cm.

-- gas filling Xe + 20% CO_2 (at the pressure of 20-30 mm) or pure propane (at the pressure of 60-80 mm).

The XTR-detector will be constructed and tested with radioactive sources at Yerevan Physics Institute (Armenia, USSR) and will be further tested and used at Fermilab. We plan to carry out initial tests at the M5 beam line in the Meson Area for determination of the individual channel response. The set-up time required is about two weeks and the total running time requested with the beam is four weeks. In Phase II we hope to set-up XTR-detector behind the 30" bubble chamber together with the other EPI detectors which are developed by the Michigan University and MIT groups.

It is to be emphasized that the XTR-detector has a very small amount of material (up to 0.8 gr/cm^2) and can be placed in the beam line without affecting the experiments downstream.

References

1. M. Aderholz, P. Lazeyras, I. Lehraus, R. Matthewson and W. Tejessy, NIM, 118, 49 (1974).
2. W.W.M. Allison, C.B. Brouks, I.N. Bunch, R.W. Fleming, and R.K. Yamamoto, NIM 133, 325 (1976).
3. Fermilab Proposals No. 327 and No. 394 (1975).
4. R.M. Sternheimer and R.F. Peierls, Phys. Rev. B3, 3581 (1974).
5. G.M. Garibian, JETP, 37, 527 (1959).
6. Fermilab Proposal No. 229 (1973).
7. K.G. Antonian, A.T. Avundzyan, S.P. Kazaryan, S.A. Kankanyan, A.G. Oganessian, and A.G. Tamanyan, Preprint EFI-130 (1975).

55c

Figure Captions

Fig. 1(a) A comparison of the relativistic rise of the most probable energy depositions at various pressures under XTR influence.

1(b) π/p ratio of ionization as a function of the momenta at the difference pressures and in the XTR-detector.

Fig. 2(a) Schematic side view of XTR-detector.

2(b) Beam diagram.

Fig. 3 Fe^{55} spectrum taken between accelerator cycles.

Fig. 4 The pulse height distributions for π and p at 40 GeV/c.

Fig. 5 The pulse height distributions for π and p at 100 GeV/c.

Fig. 6 The pulse height distributions for π and p at 200 GeV/c.

Fig. 7(a) The pulse height distributions of the mean of the smallest 6 out of 10 pulses in flux ratio $\pi/p = 1:1$ at 40 GeV/c.

Fig. 7(b) The same distributions in flux ratio $\pi/p = 10:1$.

Fig. 8 The pulse height distributions of the mean of the smallest 6 out of 10 pulses at 100 GeV/c.

Fig. 9 The pulse height distributions of the mean of the smallest 6 out of 10 pulses at 200 GeV/c.

Fig. 10 Schematic side view of Hadron Identifier Detector.

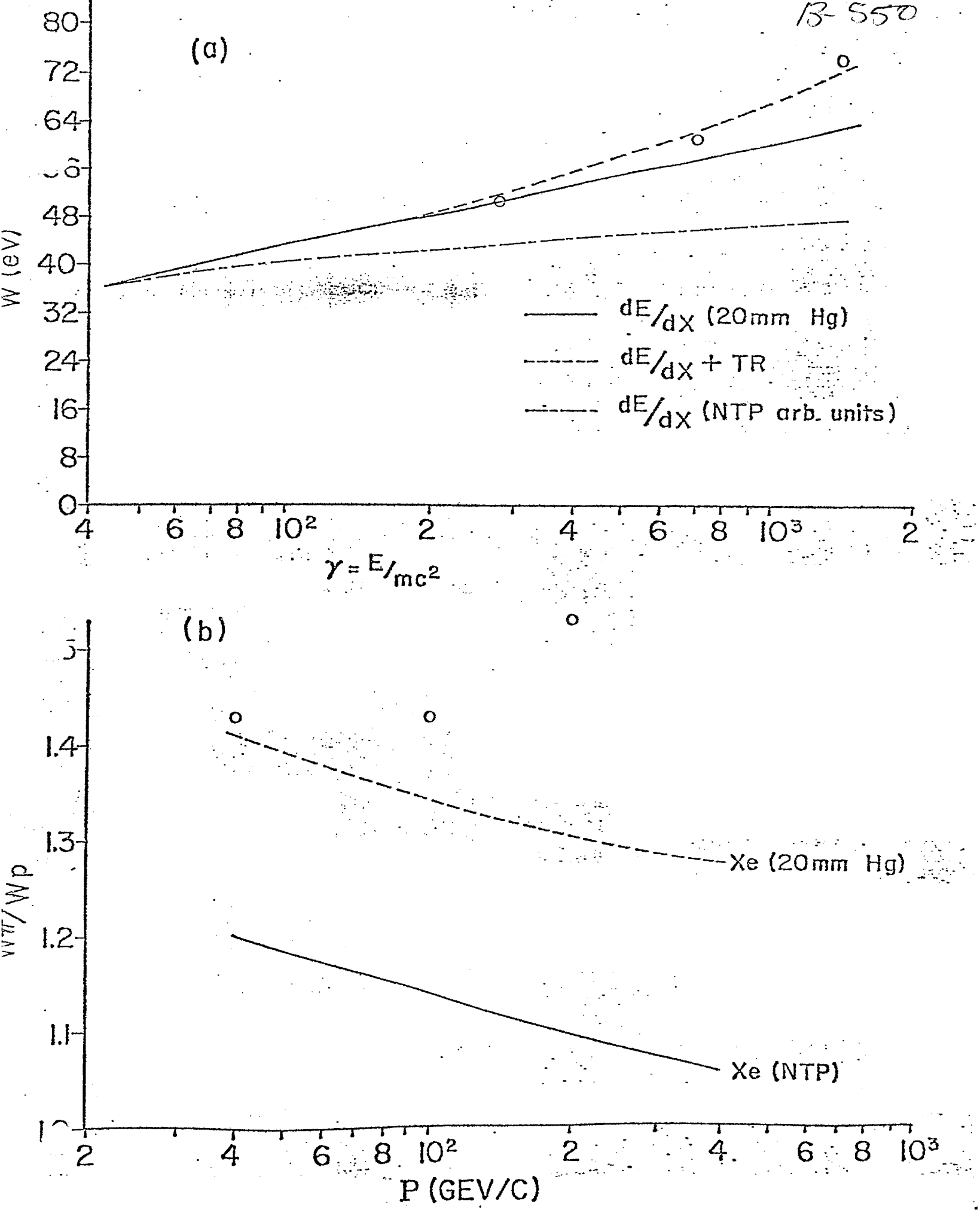
B-550
(a)
W (eV)
80
72
64
48
40
32
24
16
8
0
dE/dX (20mm Hg)
dE/dX + TR
dE/dX (NTP arb. units)
4
6
8
10²
2
4
6
8
10³
2
γ = E/mc²
(b)
1.4
1.3
1.2
1.1
Xe (20mm Hg)
Xe (NTP)
2
4
6
8
10²
2
4.
6
8
10³
P (GEV/C)

figure 1

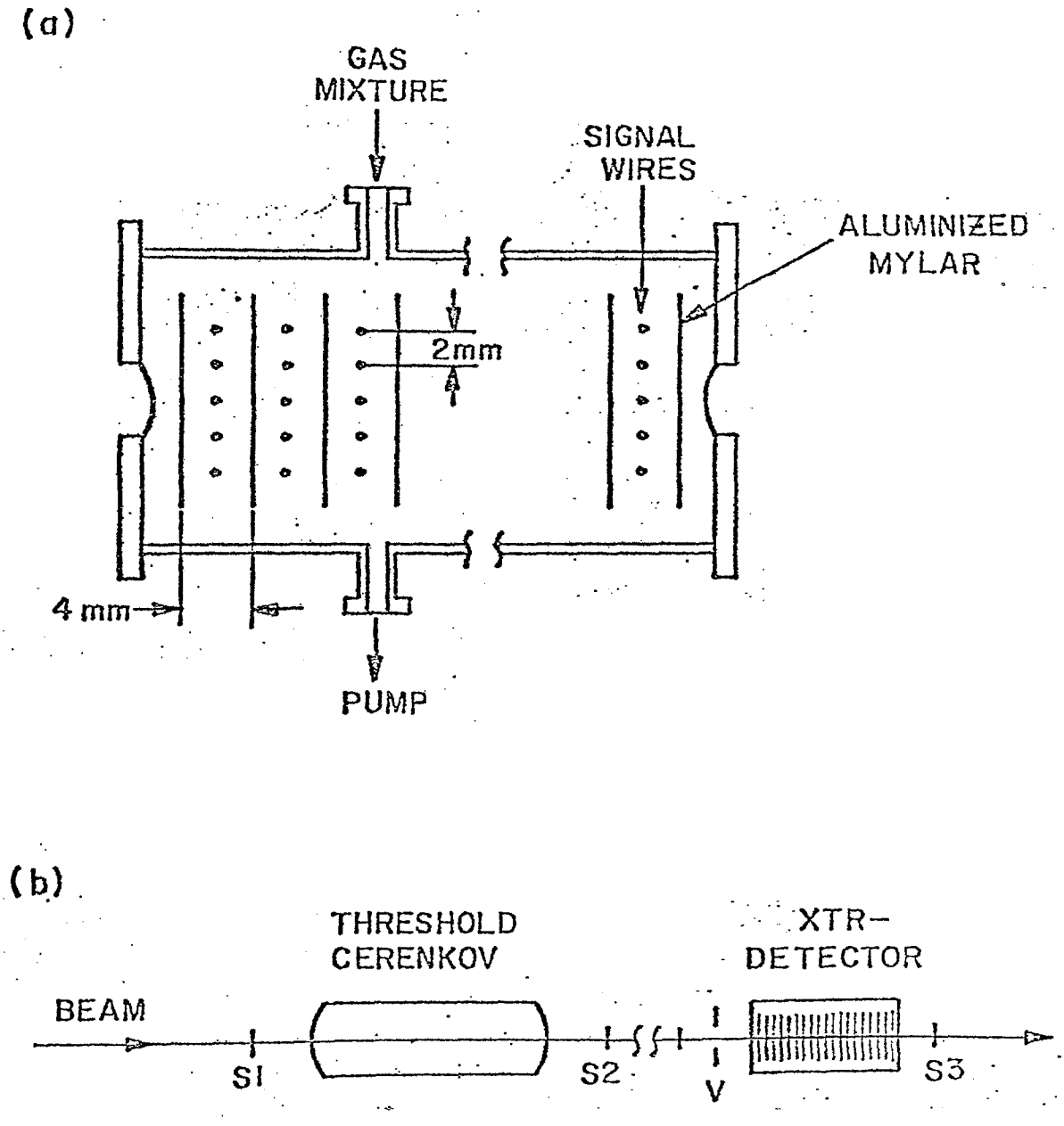
(a)
GAS
MIXTURE
SIGNAL
WIRES
ALUMINIZED
MYLAR
2mm
4 mm
PUMP
(b)
THRESHOLD
CERENKOV
XTR-
DETECTOR
BEAM
S1
S2
V
S3

Fig. 2

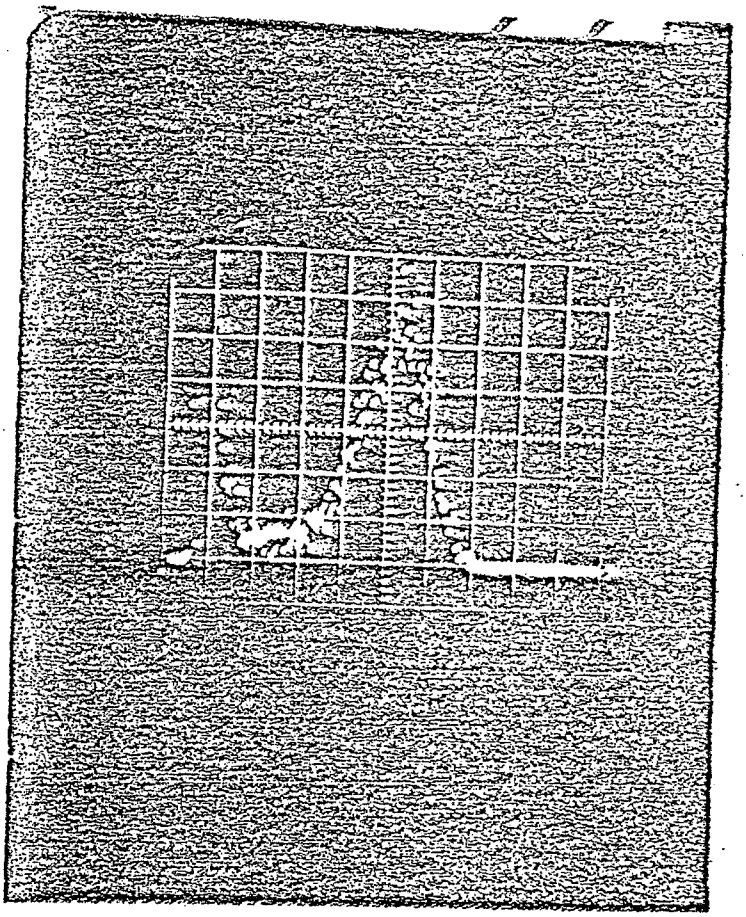

Fig. 3

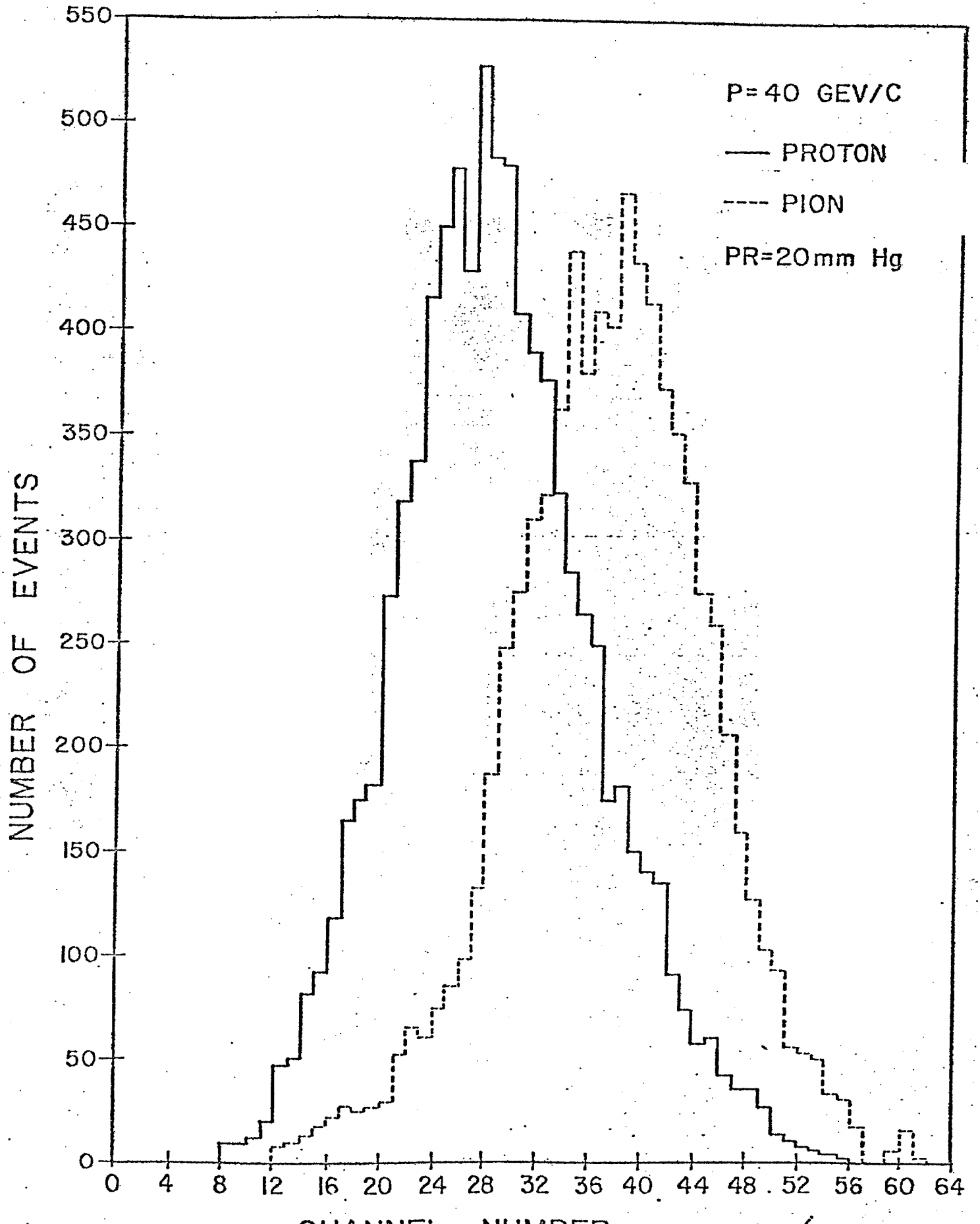
P=40 GEV/C
PROTON
PION
PR=20mm Hg
NUMBER OF EVENTS
CHANNEL NUMBER
0
50
100
150
200
250
300
350
400
450
500
550
0
4
8
12
16
20
24
28
32
36
40
44
48
52
56
60
64

Fig 4

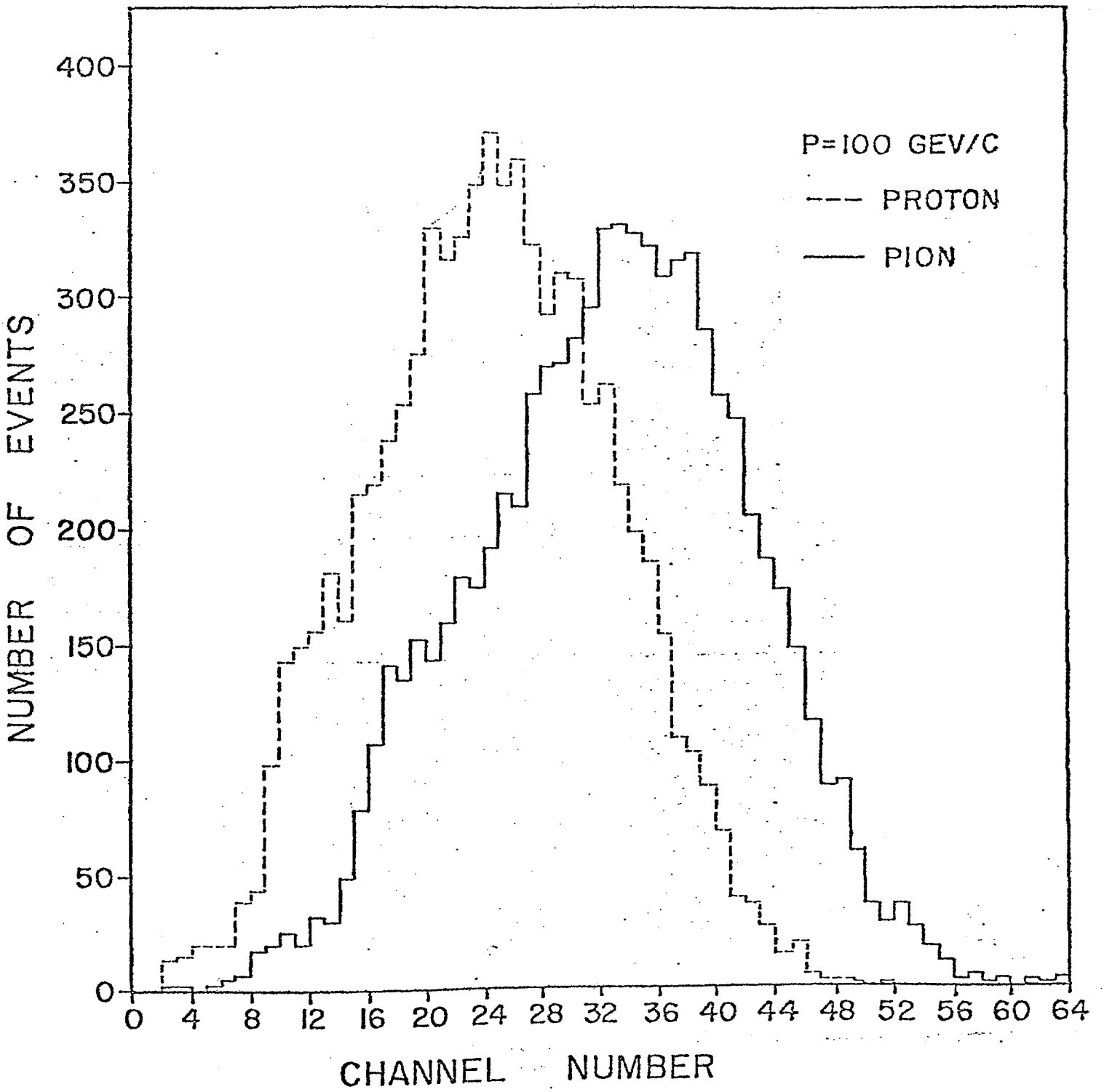
P=100 GEV/C
--- PROTON
—— PION
NUMBER OF EVENTS
0
50
100
150
200
250
300
350
400
0 4 8 12 16 20 24 28 32 36 40 44 48 52 56 60 64
CHANNEL NUMBER

Fig. 5

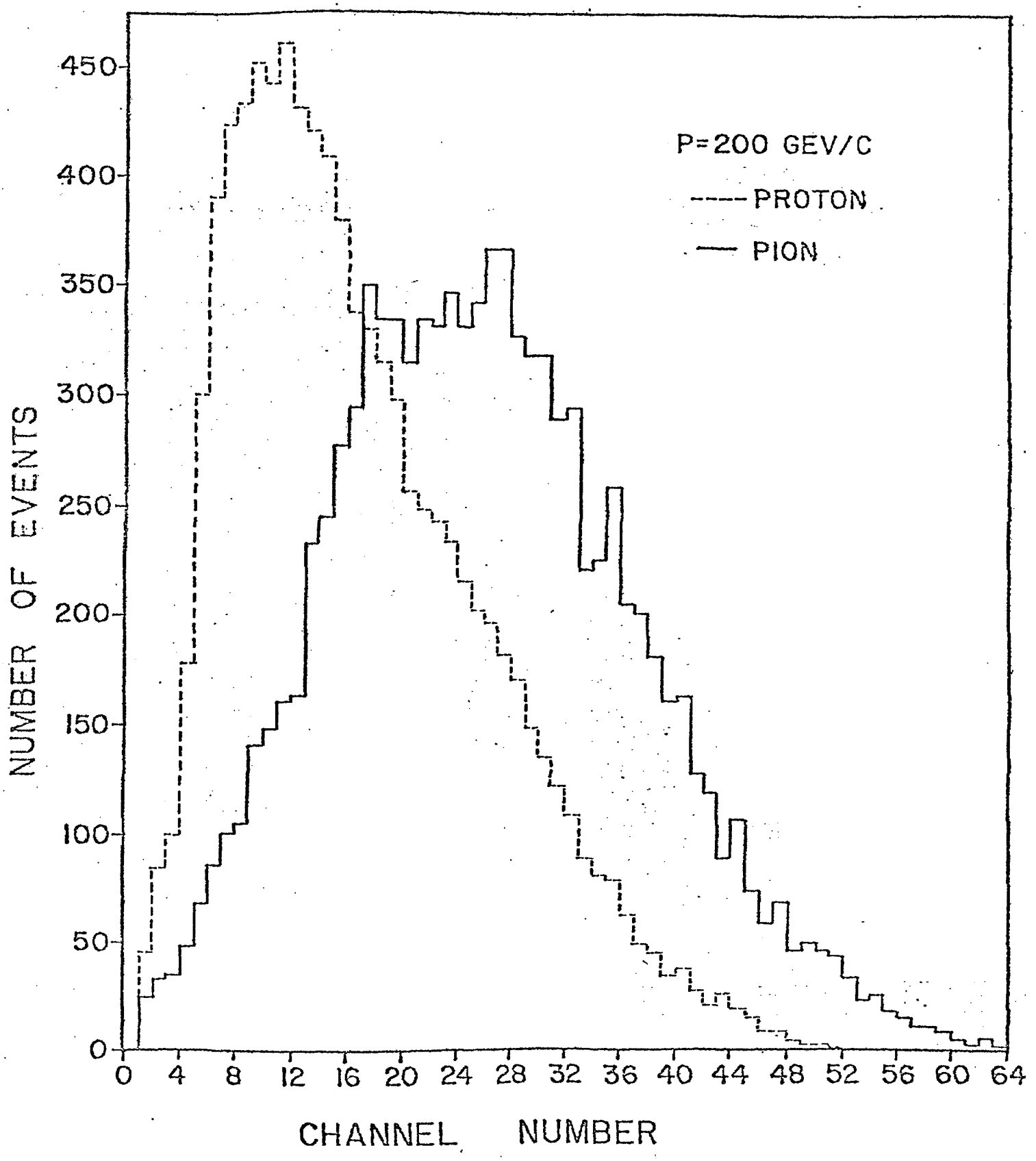
P=200 GEV/C
PROTON
PION
NUMBER OF EVENTS
0
50
100
150
200
250
300
350
400
450
0 4 8 12 16 20 24 28 32 36 40 44 48 52 56 60 64
CHANNEL NUMBER

Fig. 6

16-550

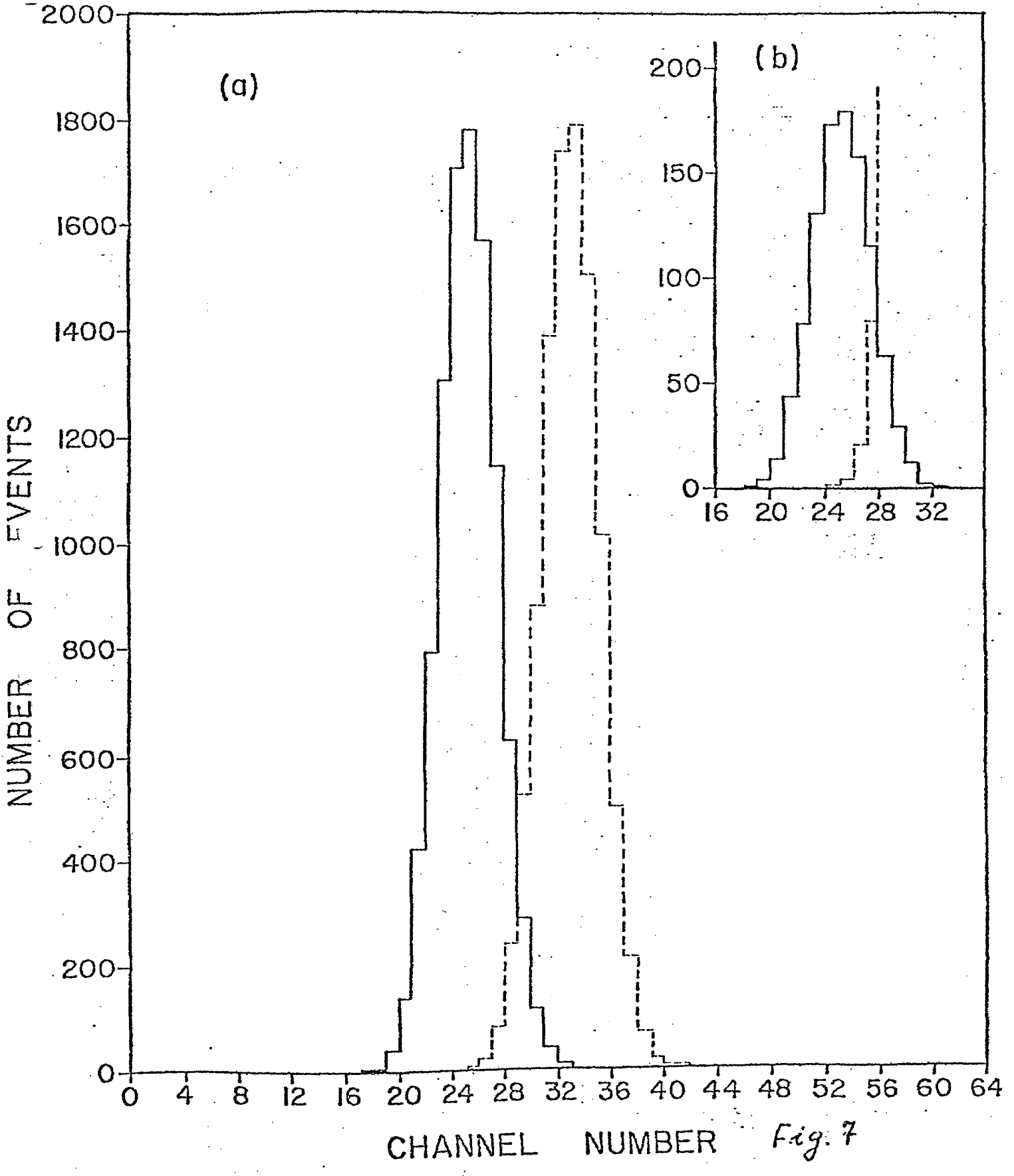
(a)
(b)
NUMBER OF EVENTS
CHANNEL NUMBER
0
200
400
600
800
1000
1200
1400
1600
1800
2000
0 4 8 12 16 20 24 28 32 36 40 44 48 52 56 60 64
0
50
100
150
200
16 20 24 28 32

Fig. 7

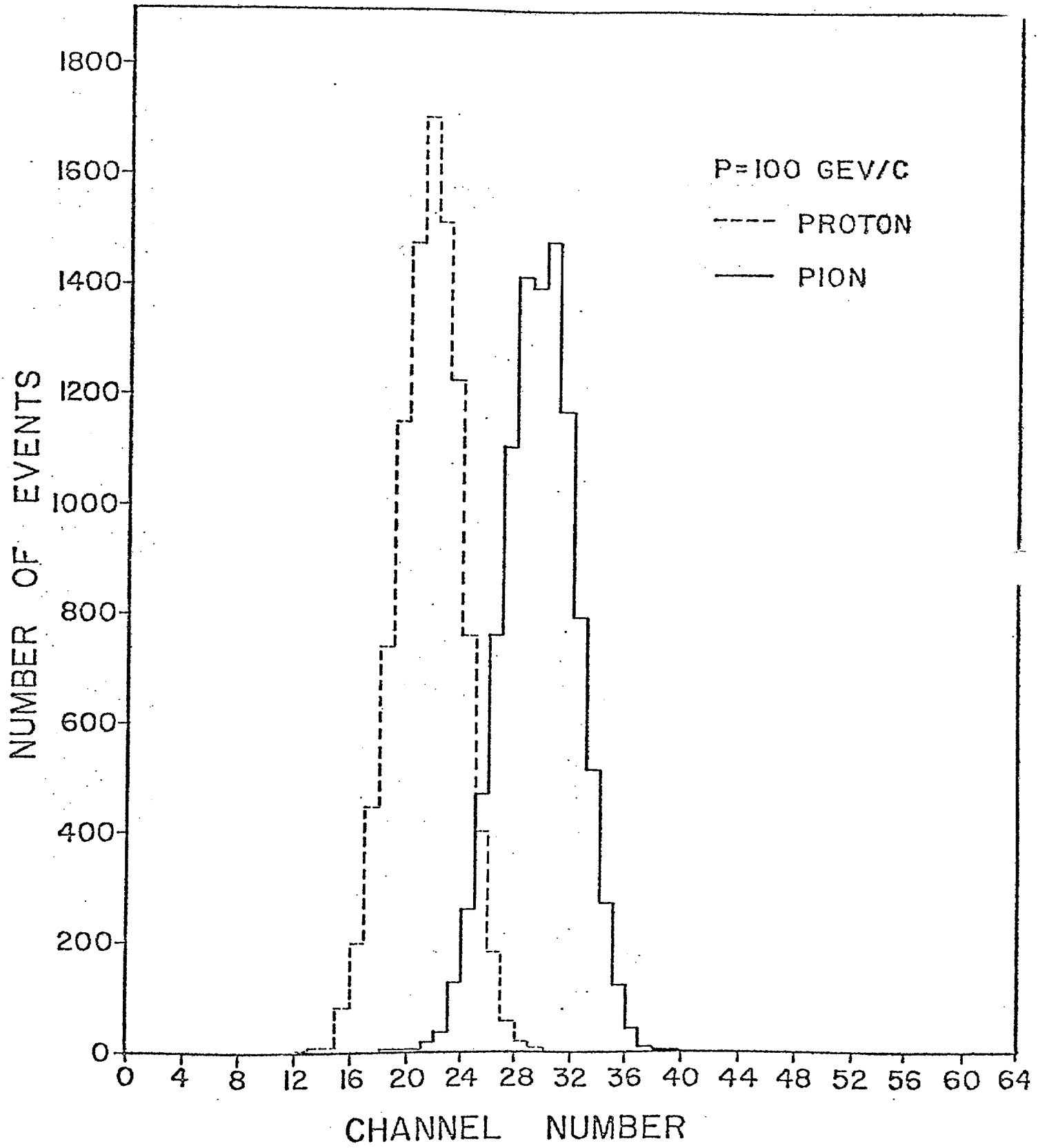
P=100 GEV/C
PROTON
PION
NUMBER OF EVENTS
1800
1600
1400
1200
1000
800
600
400
200
0
0 4 8 12 16 20 24 28 32 36 40 44 48 52 56 60 64
CHANNEL NUMBER

Fig. 8

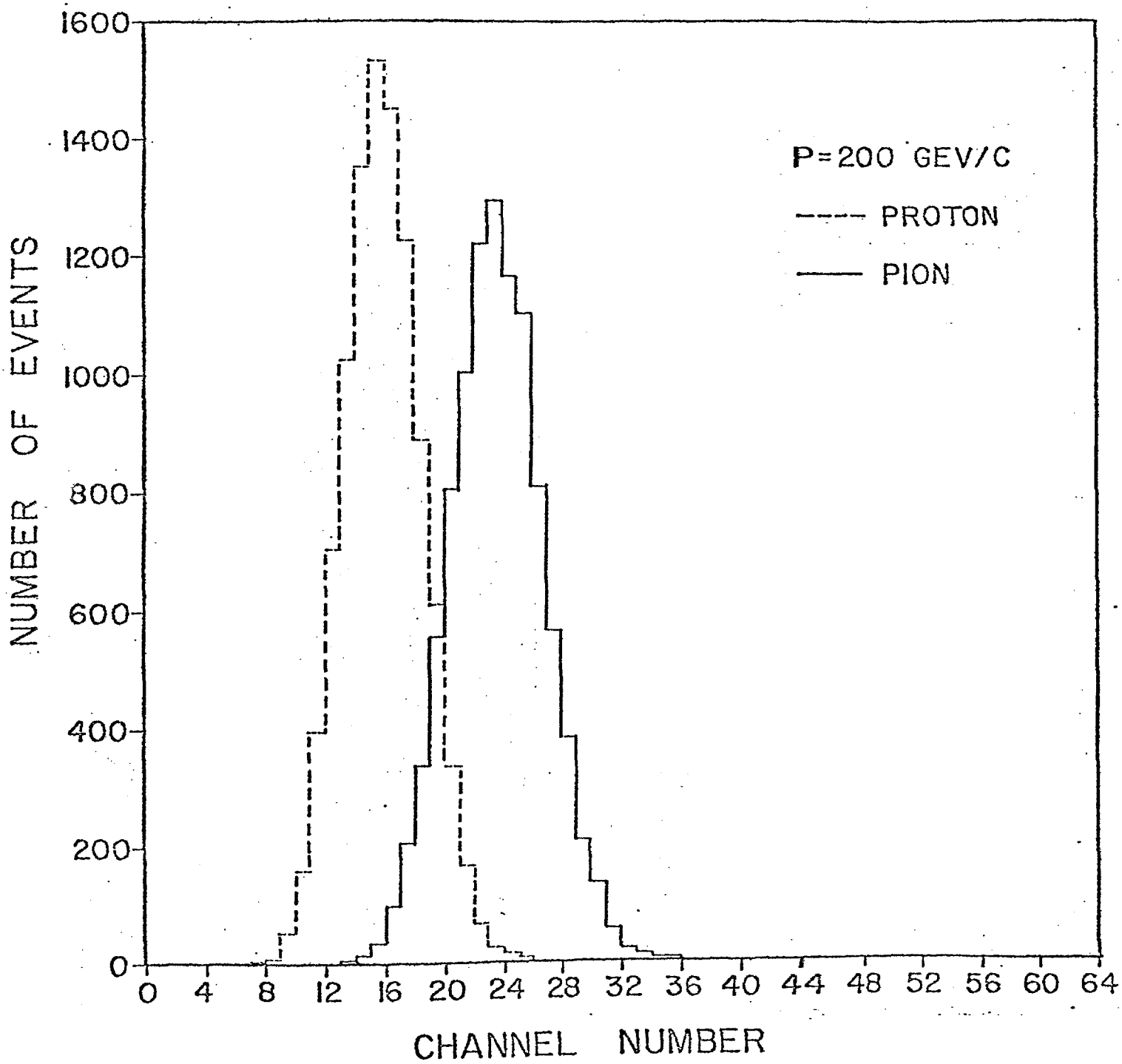
1600
1400
1200
1000
800
600
400
200
0
NUMBER OF EVENTS
P=200 GEV/C
PROTON
PION
0 4 8 12 16 20 24 28 32 36 40 44 48 52 56 60 64
CHANNEL NUMBER

Fig. 9

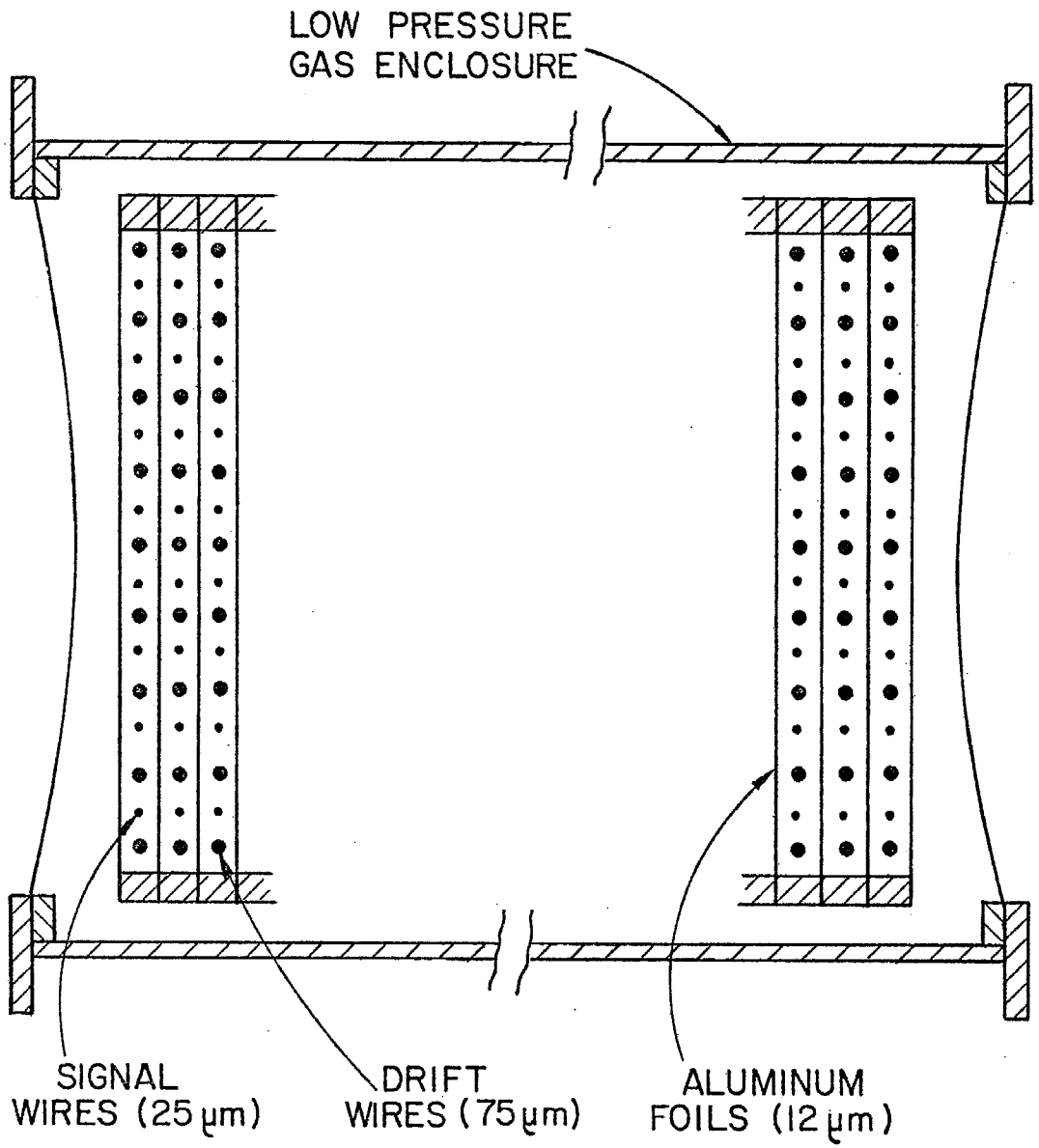
LOW PRESSURE
GAS ENCLOSURE
SIGNAL
WIRES (25 μm)
DRIFT
WIRES (75 μm)
ALUMINUM
FOILS (12 μm)

FIG. 10